Supporting Information

Stabilization of the Tensile Strength of Aged Cellulose Paper by Cholinium-amino acid Ionic Liquid Treatment

E. Scarpellini, M. Ortolani, A. Nucara, L. Baldassarre, M. Missori, R. Fastampa and R. Caminiti

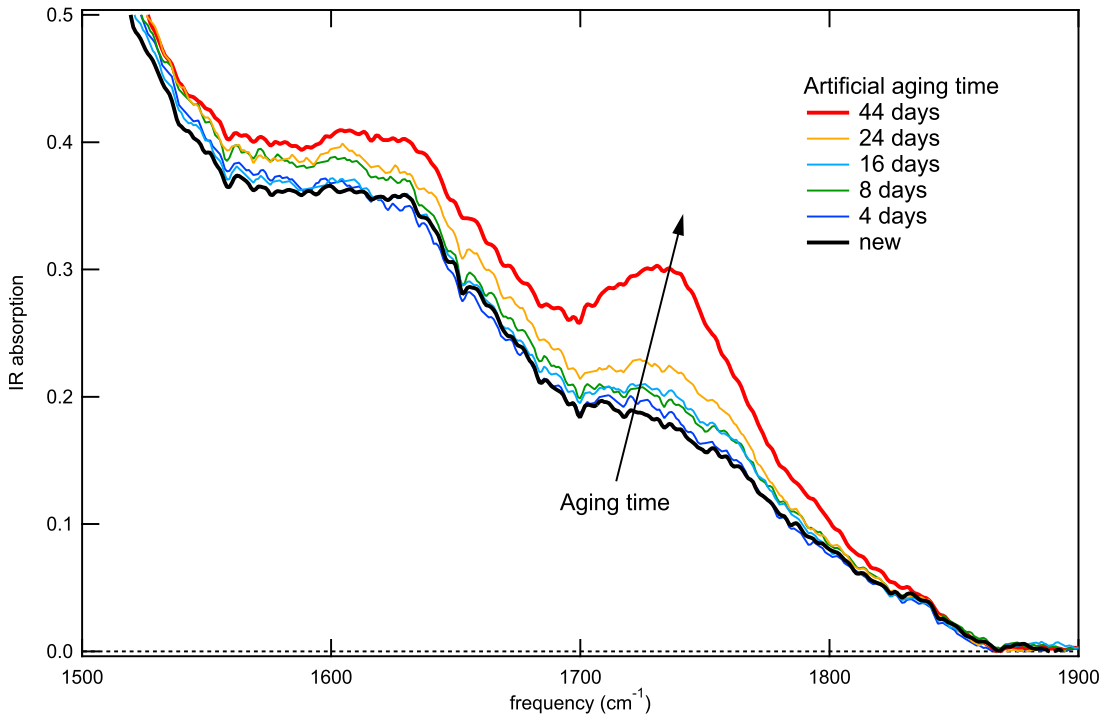

Figure R 1: Comparison between FT-IR spectra of *pristine* sample (black) and *untreated* sample aged for 4 (blue) - 8 (green) - 16 (cyan) - 24 (orange) and 44 (red) days in the carbonyl/carboxyl region.

THE JOURNAL OF PHYSICAL CHEMISTRY C

Article

pubs.acs.org/JPCC

Stabilization of the Tensile Strength of Aged Cellulose Paper by Cholinium-Amino Acid Ionic Liquid Treatment

E. Scarpellini,[†] M. Ortolani,[‡] A. Nucara,[‡] L. Baldassarre,[‡] M. Missori,[§] R. Fastampa,[‡] and R. Caminiti*[,†,∥]

[†]Department of Chemistry, Sapienza University of Rome, Piazzale Aldo Moro 5, 00185 Roma, Italy

[‡]Department of Physics, Sapienza University of Rome, Piazzale Aldo Moro 5, 00185 Roma, Italy

[§]Institute for Complex Systems, National Research Council, UOS Sapienza, Piazzale Aldo Moro 5, 00185 Roma, Italy

[∥]Research Center for Nanotechnology Applied to Engineering, Laboratory for Nanotechnologies and Nanosciences, Sapienza University of Rome, Piazzale Aldo Moro 5, 00185 Roma, Italy

Supporting Information

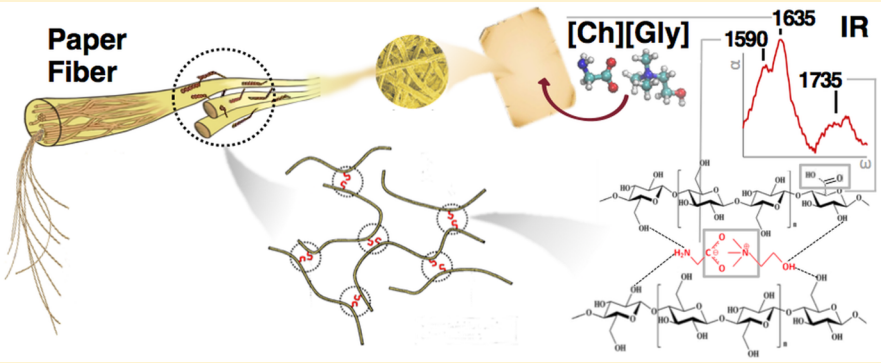

ABSTRACT: In this study, a chemical stabilization method, that preserves the tensile strength of artificially aged paper pretreated with an aqueous solution of ionic liquid, is presented. Pure cotton cellulose paper samples were soaked with cholinium glycinate ionic-liquid solution either before or after the artificial aging process, which was based on thermal degradation in dry air. The tensile strength of artificially aged paper was measured by using the double-folding technique. The role of ionic liquids was investigated by mid-infrared and terahertz time-domain absorption spectroscopy. It was found that the tensile strength of *pretreated* samples is higher than that of other aged samples. A model for changes in the cellulose structure caused by oxidation and by the binding of ionic liquid molecules is proposed, based on the analysis of the mid-infrared absorption bands in the carbonyl/carboxyl region at 1590−1750 cm^{-1}. Terahertz spectroscopy data indicate that the ionic liquid molecules penetrate in the larger size porosity, acting as binders among cellulose fibers to maintain the tensile strength of paper.

INTRODUCTION

The study of cellulose fibers, the primary and most stable component of paper, is important for a wide range of applications because of their excellent mechanical properties, which can vary significantly according to the length and size of the fibers as well as the type of chemical bonding between fibers.[1] The tensile strength of paper is the maximum force per unit width that a paper strip can resist before breaking when applying the load in the direction parallel to the strip length. The intra- and intermolecular hydrogen bonds of cellulose can influence the tensile strength of paper, as they concur to the formation of the fiber network structure, which undergoes major changes with paper aging.[2,3] Therefore, in order to developing efficient conservation techniques for cultural heritage, new methods for preservation of the cellulose fiber network structure have been developed. These methods are based on the stabilization of specific chemical bonds, leading to improvement of the elastic properties of aged paper. The strategy presented in this work is a treatment of pure cellulose paper with an aqueous solution of ionic liquid (IL). ILs can be depicted as organic salts with a melting point below 100 °C. The recent interest for ILs is mainly motivated by their possible use as "green" alternatives to synthetic organic solvents, with ILs being nonvolatile under ambient conditions. As such, ILs are being intensively investigated as a class of reaction media featuring exceptional properties like low flammability, chemical stability against air and moisture, excellent solvation potential, low water content, thermal stability, high heat capacity, high density, and high thermal conductivity. Furthermore, ILs are frequently colorless, fluid, and easy to handle. The IL used here for the treatment of cellulose paper is *cholinium glycinate* [Ch][Gly], formed by the amino acid glycine as an anion and by the organic compound choline as a cation; its chemical structure is shown in Figure 1a. This salt belongs to the

Received: July 8, 2016
Revised: October 6, 2016

DOI: 10.1021/acs.jpcc.6b06845
J. Phys. Chem. C XXXX, XXX, XXX−XXX

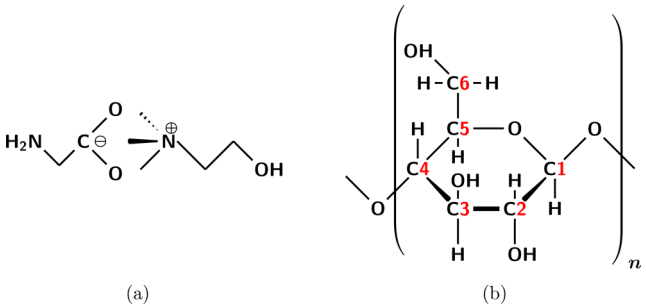

(a) (b)

Figure 1. Structures of (a) cholinium glycinate, [Ch][Gly]; (b) glucose of cellulose.

cholinium-amino acid based class of ILs. A detailed physicochemical characterization of these compounds is reported in refs 4 and 5. Moreover, choline[6,7] and glycine[8,9] have been used for the functionalization of cellulose because of the high chemical stability at high temperature (decomposition of glycine starts at T = 506 K),[10,11] and glycine may have antioxidant capacity.[12] In particular, [Ch][Gly] is used for the pretreatment of biomasses.[13] It has to be pointed out that the cholinium glycinate was found to be safe both from an environmental and healthy point of view. In this regard, the application of such a product should be encouraged in the framework of the conservation workshop, with it being totally safe for the human operators.[14−16]

Cellulose occurs in the form of long polymer chains of 1−4 linked β-D-glucose. The chemical reactions that more strongly influence the mechanical properties of cellulose occur at the hemiacetal bond, at the glycosidic linkage, and/or at the hydroxyl groups. Indeed, cellulose chains are held together into highly oriented structures (the fibers) by strong intramolecular hydrogen bonds formed by the hydroxyl groups in C2, C3, and C6 (see Figure 1b). Calculations by Tashiro and Kobayashi[17] showed that hydrogen bonds contribute about 20% of strain energy to the cellulose;[18] therefore, the mechanical properties of paper are crucially dependent on the intermolecular structure of cellulose. When the fiber is put in tension along the direction parallel to the molecular chain axis, the intermolecular hydrogen bonds suppress the torsional deformation of the flexible ether linkage and provide tensile strength to the fiber.[17] The specific local arrangement of the hydrogen bond network can result in the formation of either amorphous (chains not exactly parallel to each other) or crystalline regions (chains closely packed and parallel to each other) in different positions of the fibers. In the dense crystalline regions, cellulose chains are oriented in parallel and bonded by strong intermolecular bonds. On the contrary, the loose amorphous regions have weak interchain interactions and more hydroxyl groups exposed to oxidation and hydrolytic reactions. The crystalline domains are less reactive, and chemical reactions involving cellulose hydroxyl groups occur on the surface of crystallites and in the amorphous regions of the polymer.[19] The oxidation of cellulose corresponds to destruction of hydrogen bonds; therefore, it is a major cause of paper degradation. Oxidation reactions mainly involve the primary and secondary hydroxyl groups of the pyranose ring, which results in the creation of carbonyl (C═O) and carboxyl (—COOH) groups on the cellulose chains, inducing depolymerization of the cellulose and resulting in the decrease of tensile strength of paper.[20−24]

Natural degradation of cellulose is a very complex process of consecutive and parallel steps, which is too slow for laboratory studies. Therefore, research on cultural heritage conservation makes use of artificially accelerated aging tests, where a paper sample is subject to extreme conditions in a climate chamber, for example, at high temperature in dry air to increase the oxidation reaction rate.[25−27] Although no artificial aging method can yet reproduce the long-term degradation of paper, some artificial aging protocols showed to reproduce the distribution of many cellulose degradation byproducts,[26,28−30] and therefore, we chose these methods to determine the degradation rate of paper samples subject to a conservation treatment.

The methodology employed in this study was aimed at explaining the changes in the macroscopic tensile strength observed in folding endurance tests, by microscopic investigation of the same *new*, *pretreated*, *post-treated*, and *untreated* samples, where the word *treated* refers to immersion in the IL before (pre-) or after (post-) the artificial aging procedure. The samples were investigated from the structural point of view by scanning electron microscopy (SEM), a technique already used for the morphological study of fibers in paper.[31−33] For chemical investigation, the Fourier-transform technique (FT-IR) and terahertz time-domain spectroscopy (THz-TDS)[34] were used. FT-IR spectroscopy is commonly used in cellulose chemical characterization due to its ability to detect a specific chemical bond.

In the very far-infrared (10−100 cm^{-1}) or terahertz range (0.1−4 THz), the signatures of hydrogen bond vibrations can be observed in the absorption spectra of some classes of macromolecules, including cellulose.[35,36] It has been demonstrated that the intensity of two spectroscopic features at 2.15 and 3.03 THz can be put in relation with the degree of crystallinity of the cellulose sample. Because the wavelengths of the terahertz radiation are longer than 100 μm, i.e., much longer than the typical size of cellulose fibers and porosity of a paper sheet, a significant fraction of the terahertz radiation impinging at normal incidence on a paper sheet is transmitted without significant scattering.

Both spectroscopy techniques were used to assess the global oxidation level of cellulose and the hydrogen-bond network density, respectively.

EXPERIMENTAL SECTION

Paper Samples. Commercial Whatman filter paper n°1 pure cellulose (grammage 87 g/m^2) was used. The samples display no sizing agents or other typical paper additives (ash content 0.06% weight after combustion at 900 °C in air).

Accelerated Aging. We have chosen the International Standard Organization (ISO) 5630-1 accelerated aging method[37] in order to evaluate the consequences of the oxidation process. In the ISO 5630-1 method, the paper samples are exposed to dry heat at 105 ± 2 °C in the hot-air drying unit (oven Binder Fed 53) during the required time period. Aging times of 11 and 44 days were applied. The 11 days-aged samples have been identified as suitable for the tensile strength measurements, while the 44 days-aged samples provided a benchmark for chemical signatures of oxidation in the infrared absorption spectra.

Ionic Liquid Treatment. [Ch][Gly] was prepared in water via a potentiometric titration between choline hydroxide and the glycine amino acid which is described in ref 38. The composition was confirmed by NMR analysis and IR spectroscopy, the latter being presented in this work. A deionized aqueous solution 0.01 M IL was employed for the

DOI: 10.1021/acs.jpcc.6b06845
J. Phys. Chem. C XXXX, XXX, XXX−XXX

treatment of paper samples. The choice of the solution concentration is motivated by its pH value compatible with that of paper, also compared to the pH value obtainable with other amino acid based IL solutions. The samples were immersed for 20 min at room temperature and then let to dry in air. Samples subjected to accelerated aging for 11 days were immersed in the IL solution either before aging (*pretreated* samples) or after aging (*post-treated* samples). A nonaged sample was immersed in the same solution as a reference (*just-immersed* sample).

Folding Endurance. Folding endurance tests were carried out on all samples with the TAPPI Standard Test Method T423 with a Schopper-Type Tester.[39] Twenty sheets of each type of paper were randomly selected, and then, five folding strips of 15 × 110 mm were cut from each sheet and eventually aged and/or treated with the IL before folding endurance tests. Samples were folded across the paper's machine direction along the longitudinal fiber direction with an applied load of 1 kg.

Scanning Electron Microscopy Assets. A Field-Emission SEM Zeiss Auriga 405 workstation was used without coating of the sample, operating at an extraction potential of 8 kV, with a typical working distance of 6 mm, allowing imaging up to 4000× magnification.

Infrared Spectroscopy. A vacuum FT-IR spectrometer (Bruker IFS66v/S) equipped with a liquid-nitrogen-cooled high-sensitivity HgCdTe detector and both a transmission setup for cuvette and a specular-incidence reflection setup was used. The absorption spectra of pure IL were collected after synthesis in transmission geometry (between 600 and 2000 cm^{-1}). The IL was inserted in a liquid cell sealed by 4 mm thick wedged silicon windows to avoid degradation of the spectral resolution by Fabry−Perot interference fringes. The optical path in the IL was estimated to be around 5 μm; therefore, an approximate value of the absorption coefficient is provided. Due to high absorption from cellulose, paper samples have to be thinned mechanically before measuring them in transmission mode, and this severely impacts the sample tensile strength which is of interest here. Therefore, for measuring whole paper samples, we used the FT-IR technique in specular-reflection mode using a gold mirror as the reference channel. The procedure devised by us to retrieve the absorption spectrum of cellulose from the whole paper-sample reflectance assumes zero scattering efficiency for long wavelengths $\lambda \rightarrow \infty$ and totally homogeneous scattering (Lambertian surface scattering) for $\lambda \leq 2$ μm. This means that the measured reflectance spectrum $R(\lambda)$ is the ratio between the intrinsic cellulose extinction spectrum and the following Gaussian function[40]

$$G(\lambda) = A \exp(-\sigma^2/\lambda^2) \quad (1)$$

where A is a sample-dependent normalization factor around 0.007−0.008 and σ is a characteristic scattering object dimension which was found by best-fit to be in the range 4.0−4.5 μm for all samples, a value that well corresponds to the typical fiber dimension. Finally, the absorbance spectrum due to multipath transmission losses in the semitransparent Lambertian medium is calculated as a function of IR frequency $\omega = 2\pi c/\lambda$ (where c is the speed of light) as

$$A(\omega) = -\ln(R(\omega)\cdot G(\omega)) \quad (2)$$

which was analyzed with standard multi-Lorentzian fitting routines. In the FT-IR reflectance technique, the information on the paper sample thickness is not used and the absolute value of the absorption coefficient is therefore lost. We mention that, as a result of our procedure, the spectral weight ratio of peaks appearing in very distant spectral regions may not be comparable with that observed with, e.g., the attenuated total reflection technique, but the relative peak strength in a reduced frequency range will not be affected. In order to desorb bound water molecules, whose bending vibrations at 1645 cm^{-1} mask the carbonyl bands, the paper samples were conditioned under dynamic vacuum at 6 mbar for 24 h prior to recording the FT-IR spectra. Additionally, collecting the spectra under a vacuum prevented the samples from reabsorbing water.[41−43]

Terahertz Transmission Spectroscopy. A normal-incidence transmission THz-TDS setup (Tera K15 Menlo Systems GmbH) was employed. The broadband pulsed radiation (spectral range 0.15−3.85 THz or 5−125 cm^{-1}) emitted by a photoconductive antenna (PCA) driven by a femtosecond laser pulse[35] was focused onto the paper sheet in a 5 mm diameter spot. The transmitted pulse was recorded in the time domain with a second PCA, and the time trace was Fourier-transformed and processed to obtain the refractive index (close to 1.25 and frequency-independent for all samples, not shown) and the absorbance $\alpha(\omega)d$, where $\alpha(\omega)$ is the frequency-dependent absorption coefficient and $d \simeq 200$ μm is the paper sample thickness.

RESULTS AND DISCUSSION

Folding Endurance Tests. We measured the differences in tensile strength between 20 paper samples as provided by the maker (*new*) and paper samples cut from the same foil and artificially aged for the same duration (11 days) but with different time frames of the treatment with IL. Figure 2 shows

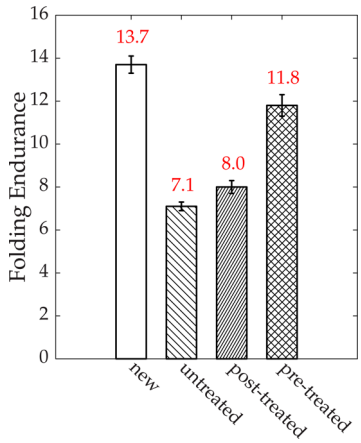

Figure 2. Measure of the tensile strength of paper through the number of double folds endured before breakage of *new* paper samples compared to those of *untreated*, *post-treated*, and *pretreated* paper samples. The values are averages over 20 measurements. All samples but the new ones were artificially aged for 11 days.

the average double-fold number before breakage of paper (folding endurance) for *new*, *untreated*, *post-treated*, and *pretreated* samples, which can be taken as a measure of their tensile strength. As expected, the new paper samples had a much higher tensile strength than the others. All aged paper samples showed a dramatic decrease of the folding endurance after 11 days of artificial aging, as is usually found in dry-heat aging processes.[29] More interestingly for this work, the *pretreated* paper samples, reaching 11.8 double folds before breakage, show a folding endurance about 40% higher than that

DOI: 10.1021/acs.jpcc.6b06845
J. Phys. Chem. C XXXX, XXX, XXX−XXX

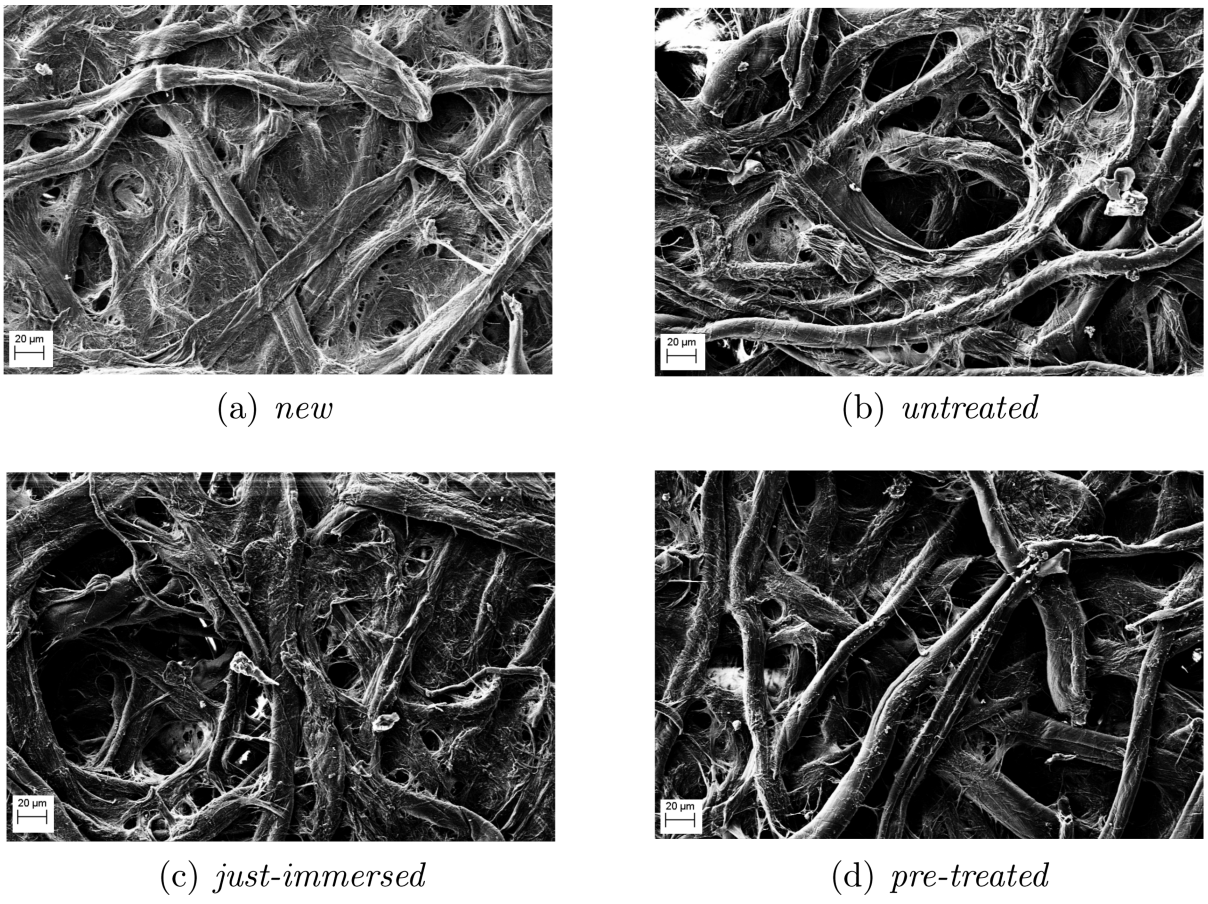

Figure 3. SEM images with a field of view of 20 μm (about 3k magnification) of new, aged, and treated paper samples.

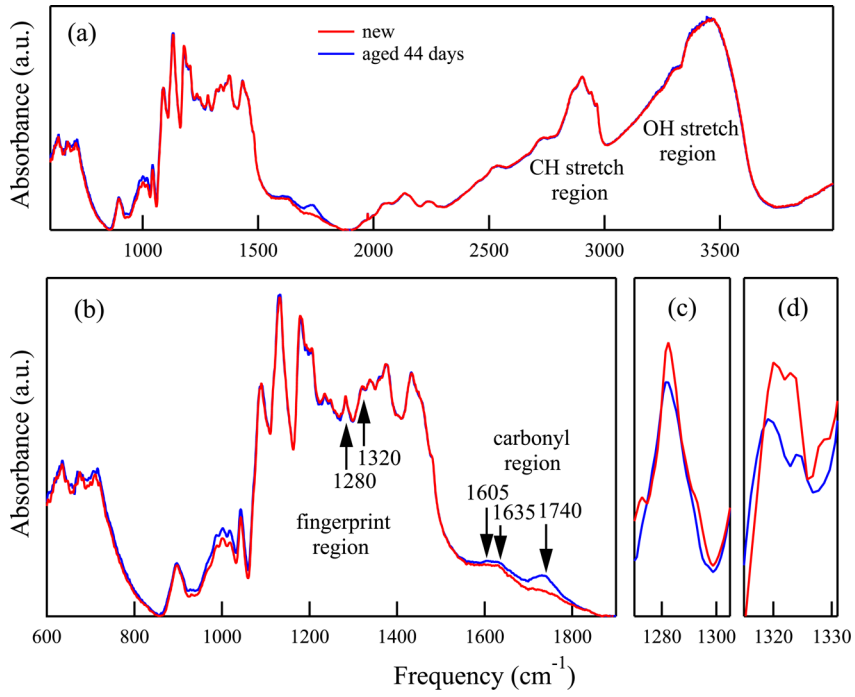

Figure 4. Comparison between FT-IR spectra of *new* sample (red) and *untreated* sample aged for 44 days (blue): (a) entire spectrum; (b) enlargement of fingerprint and carbonyl/carboxyl region; (c, d) zoom on polysaccharide peaks showing different spectral shapes with aging. Correlation of the spectral differences due to aging with the aging time which is clearly demonstrated in Figure S1, Supporting Information.

of the untreated paper (7.1 double folds) and close to that of the *new* paper (13.7 double folds). The application of IL on previously aged paper (*post-treated* sample) did not provide the same endurance increase (8.0 double folds only), indicating

DOI: 10.1021/acs.jpcc.6b06845
J. Phys. Chem. C XXXX, XXX, XXX−XXX

Table 1. Peak Wave Numbers of the Observed Bands Sensitive to Aging and Their Assignments According to the Literature

frequency (cm^{-1}), observed	frequency (cm^{-1}), in literature	reference	assignment
1282	1270	48	ring vibration plus C═O stretch
1320	1317	48, 49	CH_2 rocking vibration, C—O—H and H—C—C bending vibrations
1635	~1650	42, 44, 46	—O— tensile vibration neighboring to hydrogen atoms (conjugated carbonyl groups)
1740	1700−1750	41−43, 50, 52	—COOH stretching mode of aldehydic/carboxylic groups (only in aged samples)

that it is not simple immersion in IL that increases the tensile strength of paper. Instead, we will now show evidence that paper treatment with IL stabilizes the intermolecular bonds between cellulose chains during the artificial aging process, partially preventing tensile strength degradation.

Imaging of the Fiber Network Structure. In order to directly visualize the paper network structure, we acquired SEM image frames collected with different fields of view of 100, 20, and 10 μm. Typical target objects are expected to be just portions of the paper surface: the fiber diameter in paper cellulose is known to be 10−20 μm. The SEM images in Figure 3 show the (*new*, *untreated*, *just-immersed*, *pretreated*) paper samples before and after aging and before and after being immersed in the IL. As it can be seen comparing the different panels, no major difference in the fiber size or distribution is observed after aging or IL treatment. This fact suggests that the improved tensile strength of the *pretreated* sample must rather have a microscopic origin, related to new chemical bonds between IL and cellulose.

Infrared Characterization of Aging. The first outcome of the FT-IR analysis is the detection of the features of aging in the absorption spectra $A(\omega)$. The spectra of a *new* paper sample and a paper artificially aged for *44 days* are shown in Figure 4. Absorption bands are clearly observed at 600−700 cm^{-1} (OH out-of-plane bending),[44] ~900 cm^{-1} (β-glycosidic linkages), 1450 cm^{-1} (symmetric CH_2 bending associated with the cellulose intramolecular hydrogen bond at C_6[45]), 1590−1750 cm^{-1} (carbonyl/carboxyl region, with the stretching of the C═O bond neighboring hydrogen atoms[44,46]), 2890 cm^{-1} (C—H asymmetric and symmetric stretching[46]), and the broad peak at 3300−3500 cm^{-1} of the O—H stretching region. The region between 1300 and 900 cm^{-1} shows many strong absorption peaks and is called the "*fingerprint* region" of cellulose. Therein, peculiar stretching of C—O and C—C bonds, rocking of CH_2 and other skeletal modes, not easily encountered in other organic molecules, give their unique IR signatures.

The *fingerprint* region is magnified in Figure 4b to highlight the signatures of artificial aging. Changes in the intensity and width of spectral contribution were observed over the whole range from 900 to 1750 cm^{-1}. Two exemplar signatures of aging[47] at 1280 and 1320 cm^{-1} are highlighted in Figure 4c and d. The most prominent changes are seen in the carbonyl/carboxyl peaks, whose intensity at 1605, 1635, and 1740 cm^{-1} clearly increases (see Figure 6). In particular, the detection of a new carboxyl peak typical of oxidized cellulose at 1735 cm^{-1} is the benchmark of dry-heat aging. At the same time, no shift of the OH-band to ~3600 cm^{-1} was observed with aging, indicating that all the hydroxyl groups of cellulose are hydrogen-bonded or were oxidized, but there are no free hydroxyl terminals.[47] In Figure 4, the absorption strength of features around 1000 cm^{-1} also seems to increase with aging, but the spectral shape does not change, so this effect is not discussed because it cannot be clearly separated from small artifacts in the background subtraction procedure. A list of IR absorption peaks and bands that vary with aging is reported in Table 1.

The peaks at 1280 and 1320 cm^{-1} in Figure 4c and d, which are related to stretching, bending, and rocking of CH_2 groups, are characterized by a decrease in absorbance values with aging.[48,49] The bands at 1590−1740 cm^{-1} in Figure 4b are identified as an envelope of vibrational modes of various functional groups that vary strongly with oxidation and dehydration reactions, and therefore, it is the most suitable region for investigation of the effect of IL immersion before and after aging.[18] These functional groups are carbonyl groups (1710−1740 cm^{-1}), carboxylates (1550−1610 cm^{-1}), α-diketones and α,β-unsaturated carbonyl groups (about 1660 cm^{-1}), and C═C double bond (~1640 cm^{-1}).[42,43,50,51]

Infrared Spectrum of Cholinum Glycinate. Since the mechanism behind the paper strengthening by IL was identified thanks to FT-IR spectroscopy, it was necessary to measure the IR absorption of the IL itself. This is reported in Figure 5 and

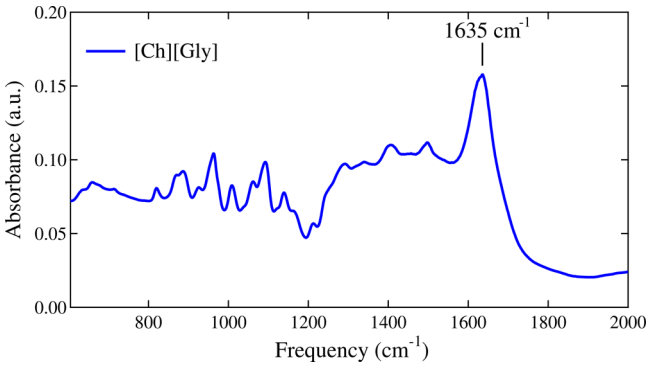

Figure 5. FT-IR absorption spectrum of the pure ionic liquid *cholinium glycinate*.

displays features that fall in the same spectral range as those of cellulose. It is possible to infer that the major contribution to the IR spectra derives from anions. As expected, in fact, such molecules are more IR-active due to the presence of the polar carboxylate group. Previously, we addressed the IR absorption spectrum of a closely related IL compound, cholinium alanynate [Ch][Ala].[4] The study of the slightly different IR absorption spectrum of [Ch][Gly] is beyond the scope of the present paper. For this reason, we have limited the spectral analysis to the region from 600 to 2000 cm^{-1}. The assignments of some of the most prominent peaks on the experimental pattern are schematically reported in Table 2. As expected, the most prominent features are due to the IR absorption from the carboxyl group around 1600 cm^{-1}. This contribution has to be carefully subtracted from the absorption spectra of paper samples treated with the IL.

Infrared Spectra of IL Treated Paper. The analysis of the absorption spectra allows a quantitative estimate of the changes introduced at the microscopic level by aging and/or by IL

DOI: 10.1021/acs.jpcc.6b06845
J. Phys. Chem. C XXXX, XXX, XXX−XXX

Table 2. Assignment of Vibrational Modes of Pure [Ch][Gly] Ionic Liquid IR Spectra[53,54]

frequency (cm^{-1})	assignment
820	HB bending
888	CN streching
961	NH_2 wagging
1092	CH_n rocking
1340	CH bending of glycine
1405	CO_2^- symmetric streching
1498	CH_3 scissoring of choline
1635	CO_2^- asymmetric stretching + NH_2 bending

treatment. To this end, we fit a multi-Lorentzian function in the carbonyl/carboxyl region (1590−1750 cm^{-1}) to the measured absorption spectra. A sample-independent background was subtracted to account for the tails of other absorption bands of cellulose. In the following analysis, the IR peak positions were fixed at values which allowed us to fit all of the spectra in Figure 6 to the same model. In other words, the IR peak position is forced not to vary with aging and/or IL treatment, in order to determine the absorption strength variation. Also, a Lorentzian peak centered at 1595 cm^{-1} was subtracted from the absorption spectra of samples immersed in the IL solution to account for direct IR absorption by the IL molecules. This contribution is assigned to the NH_2 bending of glycine,[55] shifted to lower frequency because of the hydrogen bonding with the hydroxyl group of the cellulose chain. There is no evidence of the $-NH_3^+$ peak at 1498 cm^{-1}, indicating that the compound is not dissociated but still in its ionic bond form.

The background-subtracted raw data show three well-separated carbonyl peaks at 1635, 1660, and 1735 cm^{-1}. The peak-fitting results for the *new*, *just-immersed*, *untreated*, and *pretreated* samples are reported in Figure 6. The significant line width of the carbonyl peaks seen in the raw data is indicative of the heteromorphic structure of paper. With aging, the native cellulose peak at 1635 cm^{-1} decreases in intensity, as expected. The frequency position of the peak at 1735 cm^{-1}, whose intensity increases with aging, corresponds to the IR absorption peak frequencies of expected cellulose oxidation products, as described in the literature.[18,42,43,50,51,56,57] In the artificially aged, pretreated sample in Figure 6, a shoulder at about 1660 cm^{-1} is seen, not present in the untreated sample. We can tentatively attribute this shoulder to degradation byproducts of IL (see discussion below).

The action of IL treatment before aging is detectable looking at the behavior of the spectrum of the *pretreated* sample in Figure 6. Importantly, the peak at 1735 cm^{-1}, which measures the oxidation level of cellulose, is less intense in the *pretreated* sample if compared to that of the sample aged without IL treatment. Therefore, it is reasonable to infer that the intermolecular bonds that form between [Ch][Gly] and cellulose during the artificial aging are effective in preventing cellulose oxidation. This explains the higher tensile strength of the *pretreated* paper sample. The peak at 1660 cm^{-1} instead is present only in the *pretreated* sample and not in the *post-treated* one (not shown here). Therefore, it is identified as a signature of the oxidation products of the IL molecules, which then act as *sacrificial compound* (antioxidant) by partly preventing the cellulose molecules from oxidation.

In order to highlight the correlation between cellulose oxidation and the loss of tensile strength of the paper samples, in Table 3, we plot the square of the spectral weight of the best-fit Lorentzian peak centered at 1735 cm^{-1} (the IR absorption band of oxidized cellulose) versus the quantity $\Delta N = N(\text{aged}) - N(\text{new})$, where N is the number of double folds before breakage. The difference ΔN can be taken as a measure of tensile strength loss compared to the new sample. The squared spectral weight A_{1735} is a measure of network connectivity because it is proportional to the square of the number of oxidized hydroxyl groups, which represents an estimate of the intermolecular bond loss. The correlation analysis is limited to

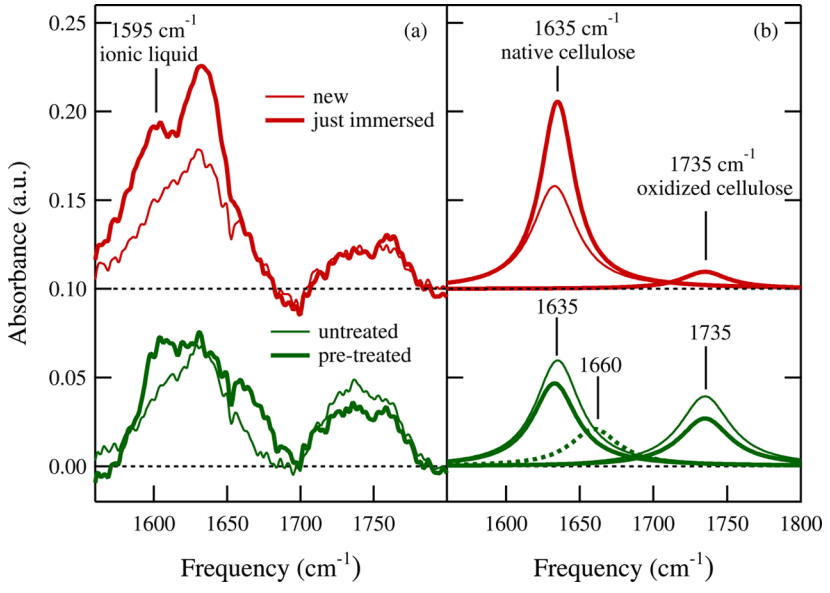

Figure 6. Results of the analysis of the IR absorption data for treated and untreated samples. The original spectra, similar to those in Figure 4, were (a) baseline-subtracted and (b) fitted to a multi-Lorentzian model. The absorption peak of IL at 1595 cm^{-1} is visible in the spectra of treated samples and was subtracted before the fitting. The peak at 1635 cm^{-1}, characteristic of native cellulose, decreases with aging in both treated and untreated samples. The oxidation peak at 1735 cm^{-1} increases with aging but less in the treated sample than in the untreated ones. In the *pretreated* sample, aging results in the appearance of a new peak at 1660 cm^{-1} identified as the oxidation product of the IL molecules acting as *sacrificial compound*.

DOI: 10.1021/acs.jpcc.6b06845
J. Phys. Chem. C XXXX, XXX, XXX−XXX

Table 3. Correlation between A_{1735}, the Squared Absorption Line Strength of the Cellulose Oxydation Peak at 1735 cm^{-1} in Figure 6, and the Tensile Strength Loss, Expressed as ΔN, the Difference in the Number of Double Folds before Breakage if Compared to the New Sample

	ΔN (number of folds)	A_{1735} (10^3 cm^{-1})
new	0	0.23717
pretreated	1.9	0.74314
untreated	6.6	1.08782

the three samples on which both types of analysis were performed, and it is indicative of the clear link between macroscopic mechanical properties of cellulose fibers and chemical bond arrangement on the microscopic scale.

Analysis of Hydrogen Bond Density by THz-TDS Measurements. Generally, hydrogen bonds do not display specific resonance frequencies in the terahertz absorption spectra of the amorphous macromolecular complex. Instead, a broad *glassy* absorption increasing as $\alpha(\omega) \sim C{\cdot}\omega^2$, where C is a numerical coefficient, is typically observed in amorphous solids[58] and biological macromolecuar complexes formed by hydrogen bond networks like solvated proteins.[59] The density of hydrogen bonds in the macromolecular complex is roughly proportional to C. In cellulose, however, due to partial crystallization, two main absorption peaks have been identified[35] at 2.15 THz, or 71 cm^{-1}, and at 3.03 THz, or 100 cm^{-1}, superimposed to the $\alpha(\omega) \sim C{\cdot}\omega^2$ background of the cellulose in the noncrystalline form. In our experiments, performed on the five samples listed in the captions of Figure 7, we clearly identified the peak at 2.15 THz and the $\alpha(\omega) \sim C{\cdot}\omega^2$ background, but we could not identify the peak at 3.03 THz because the sample transmittance was too low at that frequency. We therefore took the intensity of the peak at 2.15 THz as a measure of the degree of crystallinity[35] and the coefficient C as a measure of the density of hydrogen bonds.[59]

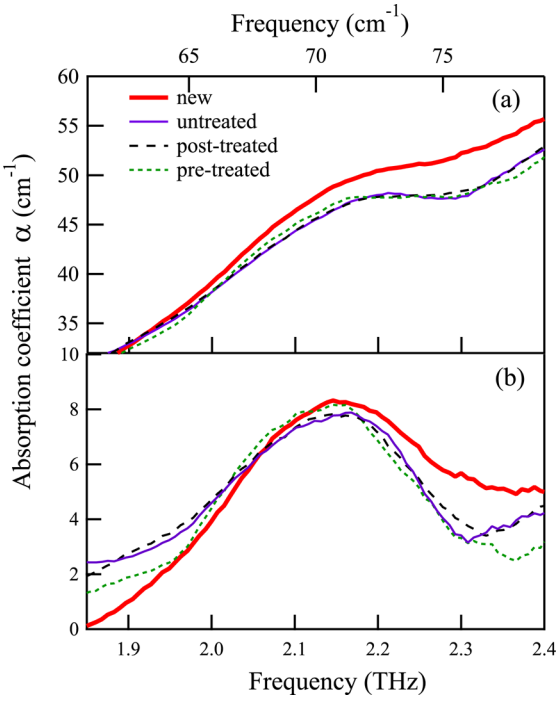

Figure 7. (a) Absorption coefficient in the THz range of the *new*, *untreated*, *post-treated*, and *pretreated* samples. (b) Absorption coefficient subtracted from the $C{\cdot}\omega^2$ background. The negligible difference among peak intensities in panel b indicates that IL treatment does not impact cellulose crystallinity.

The absorption spectrum of the *new* sample in Figure 7a displays a coefficient $C \sim 9.8$ cm^{-1}/THz^2, and the crystallinity peak at 2.15 THz is barely visible due to the high slope of the background absorption from the amorphous hydrogen bond network. In comparison, the sample artificially aged (*untreated*) has a lower slope ($C \sim 9.1$ cm^{-1}/THz^2), and therefore, the crystallinity peak at 2.15 THz becomes more visible (see Figure 7a). The intensity of the crystallinity peak, however, is unchanged with aging and/or treatment if compared to the *new* sample, indicating that the crystalline portion of cellulose seems to be unaffected by the artificial aging process. We interpret these data as a reduction of the hydrogen bond density in the amorphous cellulose network with aging. A closer look at the spectra of treated samples *pretreated* and *post-treated* shows that there is no detectable difference among their THz absorption spectra and the *untreated* one. The difference between two of these spectra and the *new* sample spectrum is shown in Figure 7b and clarifies that no change in the degree of crystallinity of cellulose is induced by treatment with IL. Also, it is clear that it does not actually prevent the degradation of the amorphous hydrogen bond network with aging. We conclude that the reduction of oxidation level of aged cellulose provided by the IL treatment and demonstrated by FT-IR spectroscopy (peak at 1735 cm^{-1}) has no direct counterpart in the reduction of the hydrogen-bond network degradation. A direct IL–cellulose intermolecular bonding process, which is stable under aging, must be sought to explain the improvement of the tensile strength of the *pretreated* sample if compared to the *post-treated* and untreated ones (see Figure 7a). Notice that no evident features can be detected in the THz spectra of *pretreated* sample. On the other hand, the presence of IL is well evident in the IR spectra. Indeed, IR penetration depth is limited at a small region below the paper surface, where IL concentration is expected to be higher probably due to steric effects. In addition, IR preferentially probes regions whose porosity have a size comparable to its wavelength (about 6 μm) where IL can easily penetrate. This information shed light on the interaction of IL and cellulose which results in being localized in the larger size accessible regions.

Model of the Action of the Ionic Liquid. The ensemble of the present experimental findings leads one to think that the [Ch][Gly] molecules statically bind to the cellulose chain. In Figure 8 is shown a probable hydrogen-bonding interaction between the nitrogen of glycine and a hydrogen of an −OH on cellulose. A hydrogen bond with glycine is also shown between an oxygen of the COO^- on glycine and the H atom of a hydroxyl group of an alcohol side chain of cellulose. This is also possible for choline hydrogen bonded with N^+ or the terminal oxygen. Water molecules may also be interposed between the fiber and the IL, which would both be hydrogen-bonded to the water molecule. The absorption of amino acids by cellulose was also demonstrated in ref 60 and by oxidized cellulose in ref 61.

The absorption process of amino acid by cellulose could be described according to the theory of localized stoichiometric adsorption and represented by Langmuir-like isotherms.[61,62]

When cellulose is oxidized, the hydrogen-bond density decreases and the extent of the penetration of reagents in the amorphous structures increases. In this context, the capability of the IL to interact with cellulose by different hydrogen bonds

DOI: 10.1021/acs.jpcc.6b06845
J. Phys. Chem. C XXXX, XXX, XXX−XXX

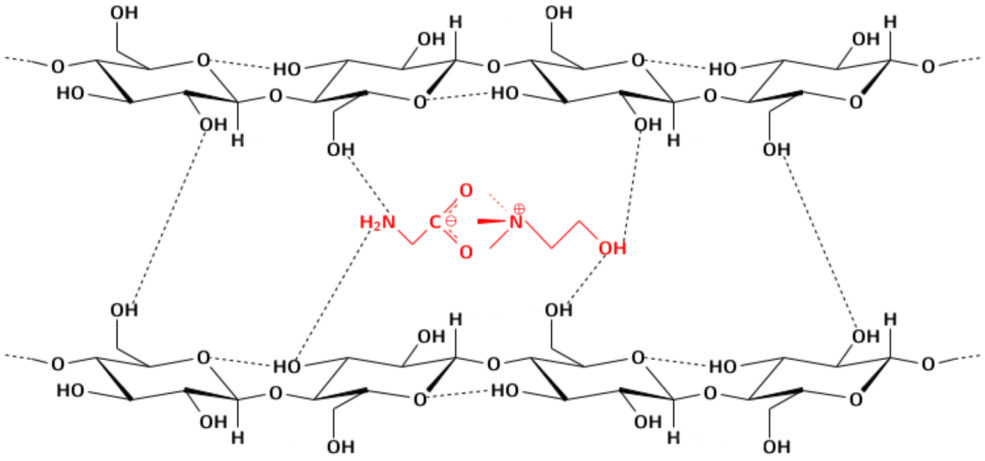

Figure 8. Plausible interaction between ionic liquid and cellulose chains.

leads to a strong IL/cellulose network that preserves the tensile strength of paper. This behavior is demonstrated here by two experimental results.

The former one is cellulose oxidation dynamics. The simple treatment of the cellulose with the IL after aging already leads to an increase of the tensile strength, although very small, as it is shown by the double fold of *post-treated* sample in Figure 2. When cellulose is partly oxidized, it contains not only the hydroxyl groups but also carboxyl and ester groups that may be hydrogen-bound to the hydroxyl, carboxyl, amide, and amine groups of the [Ch][Gly]. The *pretreated* samples, however, experienced a much higher stabilization of the tensile strength. This can be explained at the microscopic level by looking once again at the IR spectrum of the *pretreated* sample in Figure 6, which shows, beyond the already discussed increase due to oxidation under aging of the 1735 cm^{-1} peak, the appearance of a new peak at 1660 cm^{-1}. The 1660 cm^{-1} peak is compatible with vibrations of α,β-unsaturated carbonyl (C═C—C═O), C═C, or α-diketone groups, which show an IR absorbance in this range.[52,53] Since this absorption appears only in the *pretreated* sample, it is reasonable to think that it belongs to an under degradation product of IL.

Under aging, the IL molecules are therefore expected to oxidize, by capturing reactive oxygen species prone to oxidize the cellulose substrates. In summary, during aging, the IL molecules bound to cellulose chains act as *sacrificial compound* (antioxidant) for the oxidation process, preventing paper from degradation.[63]

The second fact is hydrogen-bond network degradation. Examining the terahertz absorption, one may notice that the IL does not influence the crystallinity of cellulose. In fact, in Figure 7b, the crystallinity peak of the two treated samples is essentially identical to the *untreated* one. The evident positive effect on the tensile strength of paper produced by IL treatment must then be explained in terms of diffusion of the IL molecules through the cellulose fibers and IL/cellulose intermolecular binding at larger porosity sites, as discussed above. The IL treatment does not modify the overall structure of the fiber network as confirmed by SEM imaging; rather, the presence of IL molecules between adjacent polymer chains strengthens the paper structure, partially preserving the original tensile strength.

CONCLUSIONS

In the present work, a comparison between the mechanical properties and vibrational spectra of paper samples exposed to dry-heat accelerated aging is performed. The response of the samples to an amino acid-based ionic liquid treatment was studied. The dry-heat treatment caused a loss in the tensile strength of paper, observed through a dramatic decrease of the folding endurance. The present results show that pretreatment with a ionic liquid before aging increases the tensile strength of the fiber. It is proposed that this may happen for at least two reasons: first, the ionic liquid acts as an antioxidant for the oxidation process capturing the oxygen reactive species that diffuse inside the cellulose network; second, the ionic liquid creates bonds between adjacent cellulose chains. In conclusion, the ionic liquid cholinium glycinate demonstrated significant chemical effects on paper pretreated before artificial aging, without modification of the overall cellulose fiber network structure. Ionic liquid treatment could then be considered as a sustainable method for paper-based cultural heritage conservation. Additionally, it would be of high interest to evaluate the optical effect due to the treatment of the sample with the ionic liquid. This point will be a matter of further investigation in our group. The results reported in this work may also be useful for improving the mechanical properties of devices and manufacturing products based on cellulose fibers.

ASSOCIATED CONTENT

Supporting Information

The Supporting Information is available free of charge on the ACS Publications website at DOI: 10.1021/acs.jpcc.6b06845.

Correlation of spectral differences due to aging (PDF)

AUTHOR INFORMATION

Corresponding Author

*E-mail: ruggero.caminiti@uniroma1.it. Phone: +39 06 4991 3661. Fax: +39 06 4906 31.

Notes

The authors declare no competing financial interest.

ACKNOWLEDGMENTS

The authors thank CNIS (Research Centre for Nanotechnology applied to Engineering of Sapienza University of

DOI: 10.1021/acs.jpcc.6b06845
J. Phys. Chem. C XXXX, XXX, XXX−XXX

Rome) for providing access to the scanning electron microscope within the project AWARD-Sapienza number C26H13MNEB.

REFERENCES

(1) Persson, B. N.; Ganser, C.; Schmied, F.; Teichert, C.; Schennach, R.; Gilli, E.; Hirn, U. Adhesion of Cellulose Fibers in Paper. *J. Phys.: Condens. Matter* **2013**, *25*, 045002.

(2) Strlič, M.; Kolar, J. *Ageing and Stabilisation of Paper*; National and University Library Ljubljana: Ljubljana, Slovenia, 2005.

(3) Havlínová, B.; Brezová, V.; Horňáková, L.; Mináriková, J.; Čeppan, M. Investigations of Paper Aging - A Search for Archive Paper. *J. Mater. Sci.* **2002**, *37*, 303−308.

(4) Campetella, M.; Bodo, E.; Caminiti, R.; Martino, A.; D'Apuzzo, F.; Lupi, S.; Gontrani, L. Interaction and Dynamics of Ionic Liquids Based on Choline and Amino Acid Anions. *J. Chem. Phys.* **2015**, *142*, 234502.

(5) Benedetto, A.; Bodo, E.; Gontrani, L.; Ballone, P.; Caminiti, R. Amino Acid Anions in Organic Ionic Compounds. An ab initio Study of Selected Ion Pairs. *J. Phys. Chem. B* **2014**, *118*, 2471−2486.

(6) Abbott, A. P.; Bell, T. J.; Handa, S.; Stoddart, B. Cationic Functionalisation of Cellulose Using a Choline Based Ionic Liquid Analogue. *Green Chem.* **2006**, *8*, 784.

(7) Kalaskar, D. M.; Ulijn, R. V.; Gough, J. E.; Alexander, M. R.; Scurr, D. J.; Sampson, W. W.; Eichhorn, S. J. Characterisation of Amino Acid Modified Cellulose Surfaces Using ToF-SIMS and XPS. *Cellulose* **2010**, *17*, 747−756.

(8) Chen, J.-C.; Chen, C.-C. Reaction Mechanism of Dimethyloldihydroxyethyleneurea/ Alpha-amino Acids Co-reactants on the Cross-linking of Cotton Cellulose in the Presence of Aluminum Sulfate Catalyst. *Text. Res. J.* **2007**, *77*, 843−852.

(9) Hansen, M. R.; Young, R. H. Method of Binding Particles to Fibers. New European Patent Specification ref. WO1994/004352, 1994.

(10) Dunn, M. S.; Brophy, T. W. Decomposition Points of Amino Acids. *J. Biol. Chem.* **1932**, *99*, 221−229.

(11) Yablokov, V. Y.; Smel'tsova, I. L.; Zelyaev, I. A.; Mitrofanova, S. V. Studies of the Rates of Thermal Decomposition of Glycine, Alanine, and Serine. *Russ. J. Gen. Chem.* **2009**, *79*, 1704−1706.

(12) Elizalde, B. E.; Bressa, F.; Rosa, M. D. Antioxidative Action of Maillard Reaction Volatiles: Influence of Maillard Solution Browning Level. *J. Am. Oil Chem. Soc.* **1992**, *69*, 331−334.

(13) Liu, Q.-P.; Hou, X.-D.; Li, N.; Zong, M.-H. Ionic Liquids from Renewable Biomaterials: Synthesis, Characterization and Application in the Pretreatment of Biomass. *Green Chem.* **2012**, *14*, 304−307.

(14) Ventura, S. P.; e Silva, F. A.; Gonçalves, A. M.; Pereira, J. L.; Gonçalves, F.; Coutinho, J. A. Ecotoxicity Analysis of Cholinium-based Ionic Liquids to Vibrio Fischeri Marine Bacteria. *Ecotoxicol. Environ. Saf.* **2014**, *102*, 48−54.

(15) Hou, X.-D.; Liu, Q.-P.; Smith, T. J.; Li, N.; Zong, M.-H. Evaluation of Toxicity and Biodegradability of Cholinium Amino Acids Ionic Liquids. *PLoS One* **2013**, *8*, e59145.

(16) Gouveia, W.; Jorge, T.; Martins, S.; Meireles, M.; Carolino, M.; Cruz, C.; Almeida, T.; Araújo, M. Toxicity of Ionic Liquids Prepared from Biomaterials. *Chemosphere* **2014**, *104*, 51−56.

(17) Tashiro, K.; Kobayashi, M. Theoretical Evaluation of Three-dimensional Elastic Constants of Native and Regenerated Celluloses: Role of Hydrogen Bonds. *Polymer* **1991**, *32*, 1516−1526.

(18) Fan, M.; Dai, D.; Huang, B. *Fourier Transform-Materials Analysis*; InTech: Rijeka, Croatia, 2012; pp 45−68.

(19) Varshney, V.; Naithani, S. *Cellulose Fibers: Bio-and Nano-Polymer Composites*; Springer: Germany, 2011; pp 43−60.

(20) Łojewski, T.; Miśkowiec, P.; Missori, M.; Lubańska, A.; Proniewicz, L.; Łojewska, J. FTIR and UV/vis as Methods for Evaluation of Oxidative Degradation of Model Paper: DFT Approach for Carbonyl Vibrations. *Carbohydr. Polym.* **2010**, *82*, 370−375.

(21) Łojewski, T.; Zięba, K.; Knapik, A.; Bagniuk, J.; Lubańska, A.; Łojewska, J. Evaluating Paper Degradation Progress. Cross-linking between Chromatographic, Spectroscopic and Chemical Results. *Appl. Phys. A: Mater. Sci. Process.* **2010**, *100*, 809−821.

(22) Corsaro, C.; Mallamace, D.; Łojewska, J.; Mallamace, F.; Pietronero, L.; Missori, M. Molecular Degradation of Ancient Documents Revealed by ^{1}H HR-MAS NMR spectroscopy. *Sci. Rep.* **2013**, *3*, 2896.

(23) Conte, A. M.; Pulci, O.; Misiti, M.; Łojewska, J.; Teodonio, L.; Violante, C.; Missori, M. Visual Degradation in Leonardo da Vinci's Iconic Self-portrait: A Nanoscale Study. *Appl. Phys. Lett.* **2014**, *104*, 224101.

(24) Missori, M.; Pulci, O.; Teodonio, L.; Violante, C.; Kupchak, I.; Bagniuk, J.; Łojewska, J.; Conte, A. M. Optical Response of Strongly Absorbing Inhomogeneous Materials: Application to Paper Degradation. *Phys. Rev. B: Condens. Matter Mater. Phys.* **2014**, *89*, 054201.

(25) Bansa, H. Accelerated Ageing of Paper: Some Ideas on its Practical Benefit. *Restaurator* **2002**, *23*, 106−117.

(26) Porck, H. J. *Rate of Paper Degradation: the Predictive Value of Artificial Aging Tests*; European Commission on Preservation and Access: Amsterdam, The Netherlands, 2000.

(27) Van Der Reyden, D. Recent Scientific Research in Paper Conservation. *J. Am. Inst. Conserv.* **1992**, *31*, 117−138.

(28) Batterham, I.; Rai, R. A Comparison of Artificial Ageing with 27 Years of Natural Ageing. AICCM Book, Paper and Photographic Materials Symposium. Australia, 2008; pp 81−89.

(29) Karlovits, M.; Gregor-Svetec, D. Durability of Cellulose and Synthetic Papers Exposed to Various Methods of Accelerated Ageing. *Acta Polytech. Hung.* **2012**, *9*, 81−100.

(30) Łojewski, T.; Miśkowiec, P.; Molenda, M.; Lubańska, A.; Łojewska, J. Artificial Versus Natural Ageing of Paper. Water Role in Degradation Mechanisms. *Appl. Phys. A: Mater. Sci. Process.* **2010**, *100*, 625−633.

(31) Manso, M.; Carvalho, M. L. Application of Spectroscopic Techniques for the Study of Paper Documents: A Survey. *Spectrochim. Acta, Part B* **2009**, *64*, 482−490.

(32) Michaelsen, A.; Piñar, G.; Pinzari, F. Molecular and Microscopical Investigation of the Microflora Inhabiting a Deteriorated Italian Manuscript Dated from the Thirteenth Century. *Microb. Ecol.* **2010**, *60*, 69−80.

(33) Piñar, F.; Tafer, G.; Sterflinger, H.; Pinzari, K. Amid the Possible Causes of a Very Famous Foxing: Molecular and Microscopic Insight into Leonardo da Vinci's Self-portrait. Environ. *Environ. Microbiol. Rep.* **2015**, *7*, 849−859.

(34) El Haddad, J.; de Miollis, F.; Bou Sleiman, J.; Canioni, L.; Mounaix, P.; Bousquet, B. Chemometrics Applied to Quantitative Analysis of Ternary Mixtures by Terahertz Spectroscopy. *Anal. Chem.* **2014**, *86*, 4927−4933.

(35) Vieira, F. S.; Pasquini, C. Determination of Cellulose Crystallinity by Terahertz-time Domain Spectroscopy. *Anal. Chem.* **2014**, *86*, 3780−3786.

(36) Kurabayashi, T.; Suzuki, K.; Yodokawa, S.; Kosaka, S.; Ando, K. Identification of Cellulosic Fiber by Terahertz Spectroscopy. 2012 37th International Conference on Infrared, Millimeter, and Terahertz Waves. University of Wollongong, Wollongong, NSW, Australia, 2012.

(37) International and Organization for Standardization, *Paper and Board − Accelerated Ageing − Part 1: Dry Heat Treatment at 105 degrees C*; ISO 5630-1:1991, 1991.

(38) De Santis, S.; Masci, G.; Casciotta, F.; Caminiti, R.; Scarpellini, E.; Campetella, M.; Gontrani, L. Cholinium-amino acid Based Ionic Liquids: a New Method of Synthesis and Physico-chemical Characterization. *Phys. Chem. Chem. Phys.* **2015**, *17*, 20687−20698.

(39) Lindström, T.; Fellers, C.; Iversen, T.; Nilsson, T.; Rigdahl, M. *Ageing/Degradation of Paper*; National Archives of Sweden; Royal Library: Stockholm, Sweden, 1989.

(40) Ortolani, M.; Lee, J.; Schade, U.; Hübers, H.-W. Surface Roughness Effects on the Terahertz Reflectance of Pure Explosive Materials. *Appl. Phys. Lett.* **2008**, *93*, 081906.

(41) Łojewska, J.; Miśkowiec, P.; Łojewski, T.; Proniewicz, L. Cellulose Oxidative and Hydrolytic Degradation: In situ FTIR Approach. *Polym. Degrad. Stab.* **2005**, *88*, 512−520.

(42) Łojewska, J.; Lubańska, A.; Łojewski, T.; Miśkowiec, P.; Proniewicz, L. Kinetic Approach to Degradation of Paper. In situ FTIR

DOI: 10.1021/acs.jpcc.6b06845
J. Phys. Chem. C XXXX, XXX, XXX−XXX

Transmission Studies on Hydrolysis and Oxidation. *e-Preserv. Sci.* **2005**, *2*, 1−12.
(43) Ali, M.; Emsley, A.; Herman, H.; Heywood, R. Spectroscopic Studies of the Ageing of Cellulosic Paper. *Polymer* **2001**, *42*, 2893−2900.
(44) Toğrul, H.; Arslan, N. Flow Properties of Sugar Beet Pulp Cellulose and Intrinsic Viscosity-Molecular Weight Relationship. *Carbohydr. Polym.* **2003**, *54*, 63−71.
(45) Kumar, V.; De La Luz Reus-Medina, M.; Yang, D. Preparation, Characterization, and Tabletting Properties of a New Cellulose-based Pharmaceutical Aid. *Int. J. Pharm.* **2002**, *235*, 129−140.
(46) Azubuike, C. P.; Rodríguez, H.; Okhamafe, A. O.; Rogers, R. D. Physicochemical Properties of Maize Cob Cellulose Powders Reconstituted from Ionic Liquid Solution. *Cellulose* **2012**, *19*, 425−433.
(47) Kondo, T. The Assignment of IR Absorption Bands due to Free Hydroxyl Groups in Cellulose. *Cellulose* **1997**, *4*, 281−292.
(48) Schwanninger, M.; Rodrigues, J.; Pereira, H.; Hinterstoisser, B. Effects of Short-time Vibratory Ball Milling on the Shape of FT-IR Spectra of Wood and Cellulose. *Vib. Spectrosc.* **2004**, *36*, 23−40.
(49) Proniewicz, L. M.; Paluszkiewicz, C.; Wesełucha-Birczyńska, A.; Majcherczyk, H.; Barański, A.; Konieczna, A. FT-IR and FT-Raman Study of Hydrothermally Degradated Cellulose. *J. Mol. Struct.* **2001**, *596*, 163−169.
(50) Łojewska, J.; Lubańska, A.; Miśkowiec, P.; Łojewski, T.; Proniewicz, L. FTIR in situ Transmission Studies on the Kinetics of Paper Degradation via Hydrolytic and Oxidative Reaction Paths. *Appl. Phys. A: Mater. Sci. Process.* **2006**, *83*, 597−603.
(51) Bronzato, M.; Calvini, P.; Federici, C.; Dupont, A.-L.; Meneghetti, M.; Di Marco, V.; Biondi, B.; Zoleo, A. Degradation By-products of Ancient Paper Leaves from Wash Waters. *Anal. Methods* **2015**, *7*, 8197−8205.
(52) Calvini, P.; Gorassini, A. FTIR-Deconvolution Spectra of Paper Documents. *Restaurator* **2002**, *23*, 48−66.
(53) Lin-Vien, D.; Colthup, N. B.; Fateley, W. G.; Grasselli, J. G. *The Handbook of Infrared and Raman Characteristic Frequencies of Organic Molecules*; Elsevier: Amsterdam, The Netherlands, 1991.
(54) Wakelyn, P. J. Quaternary Ammonium Salts as Antistatic Agents on Polyacrylonitrile Fibers. Thesis, School of Polymer, Textile and Fiber Engineering Theses and Dissertations, 1967.
(55) Stepanian, S.; Reva, I.; Radchenko, E.; Rosado, M.; Duarte, M.; Fausto, R.; Adamowicz, L. Matrix-isolation Infrared and Theoretical Studies of the Glycine Conformers. *J. Phys. Chem. A* **1998**, *102*, 1041−1054.
(56) Calvini, P.; Gorassini, A.; Luciano, G.; Franceschi, E. FTIR and WAXS Analysis of Periodate Oxycellulose: Evidence for a Cluster Mechanism of Oxidation. *Vib. Spectrosc.* **2006**, *40*, 177−183.
(57) Calvini, P.; Silveira, M. FTIR Analysis of Naturally Aged $FeCl_3$ and $CuCl_2$-doped Cellulose Papers. *e-Preserv. Sci.* **2008**, *5*, 1−6.
(58) Bagdad, W.; Stolen, R. Far Infrared Absorption in Fused Quartz and Soft Glass. *J. Phys. Chem. Solids* **1968**, *29*, 2001−2008.
(59) Xu, J.; Plaxco, K. W.; Allen, S. J. Probing the Collective Vibrational Dynamics of a Protein in Liquid Water by Terahertz Absorption Spectroscopy. *Protein Sci.* **2006**, *15*, 1175−1181.
(60) Salas, C.; Rojas, O. J.; Lucia, L. a.; Hubbe, M. a.; Genzer, J. Adsorption of Glycinin and β-conglycinin on Silica and Cellulose: Surface Interactions as a Function of Denaturation, pH, and Electrolytes. *Biomacromolecules* **2012**, *13*, 387−396.
(61) Zimnitsky, D. S.; Yurkshtovich, T. L.; Bychkovsky, P. M. Adsorption of Zwitterionic Drugs onto Oxidized Cellulose. *J. Colloid Interface Sci.* **2006**, *295*, 33−40.
(62) Senō, M.; Yamabe, T. Ion-exchange Behavior of Acidic and Basic Amino Acids. *Bull. Chem. Soc. Jpn.* **1961**, *34*, 1021−1026.
(63) Missori, M.; Righini, M.; Dupont, A.-L. Gelatine Sizing and Discoloration: A Comparative Study of Optical Spectra Obtained from Ancient and Artificially Aged Modern Papers. *Opt. Commun.* **2006**, *263*, 289−294.

DOI: 10.1021/acs.jpcc.6b06845
J. Phys. Chem. C XXXX, XXX, XXX−XXX